How to cite: *Angew. Chem. Int. Ed.* **2023**, *62*, e202315085
doi.org/10.1002/anie.202315085

Polymer Recycling | Hot Paper

Thermally Robust yet Deconstructable and Chemically Recyclable High-Density Polyethylene (HDPE)-Like Materials Based on Si–O Bonds

*Alayna M. Johnson and Jeremiah A. Johnson**

Abstract: Polyethylene (PE) is the most widely produced synthetic polymer. By installing chemically cleavable bonds into the backbone of PE, it is possible to produce chemically deconstructable PE derivatives; to date, however, such designs have primarily relied on carbonyl- and olefin-related functional groups. Bifunctional silyl ethers (BSEs; $SiR_2(OR'_2)$) could expand the functional scope of PE mimics as they possess strong Si–O bonds and facile chemical tunability. Here, we report BSE-containing high-density polyethylene (HDPE)-like materials synthesized through a one-pot catalytic ring-opening metathesis polymerization (ROMP) and hydrogenation sequence. The crystallinity of these materials can be adjusted by varying the BSE concentration or the steric bulk of the Si-substituents, providing handles to control thermomechanical properties. Two methods for chemical recycling of HDPE mimics are introduced, including a circular approach that leverages acid-catalyzed Si–O bond exchange with 1-propanol. Additionally, despite the fact that the starting HDPE mimics were synthesized by chain-growth polymerization (ROMP), we show that it is possible to recover the molar mass and dispersity of recycled HDPE products using step-growth Si–O bond formation or exchange, generating high molecular weight recycled HDPE products with mechanical properties similar to commercial HDPE.

Introduction

Polyethylene (PE) is the most widely-produced thermoplastic in the world, comprising more than 60 % of the total plastic content in the municipal solid waste (MSW) stream.[1] Approximately 100 million tons of PE are produced annually for numerous applications, including food packaging, plastic bottles, and grocery bags.[2] While PE thermoplastics are recyclable via melt-processing in principle, their presence in multi-component materials and mixed waste streams makes traditional recycling costly in practice. Moreover, PE is difficult to chemically recycle to monomers due to its high ceiling temperature ($>600\,^{\circ}C$),[3] and while pyrolysis or post-polymerization modification of PE can be used to generate useful chemical building blocks or alternative materials, such strategies may create new waste streams and not reduce reliance on virgin PE.[4,5] Thus, strategies to break down PE-based materials and demonstrate that the products of such processes can be repolymerized back into PE-like materials with equivalent properties may be desirable.

The installation of selectively cleavable bonds within the backbone of linear, high-density PE (HDPE) represents a common strategy to achieve deconstructable "PE mimics" with potential routes for chemical recycling and/or environmental deconstructability.[6,7] Such materials can be synthesized via post-polymerization modification of HDPE or through de novo syntheses; if designed correctly, they can display many of the key structural and performance features of conventional HDPE. Thus, such mimics could replace HDPE in applications where their additional cost of manufacturing is tolerable (e.g., electronics, coatings, or medical devices) and where triggered chemical deconstructability may be desirable.

The concept of spacing functional groups along the backbone of hydrocarbon segments to obtain materials with PE-like properties can be traced conceptually back to 1940 (i.e., before the widespread development of HDPE), when Carothers reported that polyesters and polyamides containing long-chain aliphatic segments displayed higher degrees of crystallinity, higher melting temperatures, greater hydrophobicity, and increased stiffness as the length of the aliphatic segments increased.[8] Building on this general principle, many HDPE-like materials have been synthesized, typically via step-growth polymerization reactions (e.g., polycondensation or acyclic diene metathesis polymerization).[7,9–17] Less attention has been paid to the synthesis of such materials using chain polymerizations, despite the fact that most HDPE is synthesized using such mechanisms.[18] A few examples of PE mimics prepared via ring-opening metathesis polymerization (ROMP) have been reported; however, chemical recycling of such polymers has not, to our knowledge, been demonstrated.[19–21] Furthermore, regardless of whether step-growth or chain-growth

[*] A. M. Johnson, J. A. Johnson
Department of Chemistry, Massachusetts Institute of Technology
77 Massachusetts Avenue, Cambridge, MA 02139 (USA)
E-mail: jaj2019@mit.edu

mechanisms are used, the cleavable bonds introduced into PE and PE-like materials have so far been based primarily on C–O (e.g., esters, orthoesters, and carbonates) and C=C bonds, which offer a limited range of selective cleavage reactions and in some cases may introduce hydrolytic, photo, and/or thermal instability.[9,19,22–31] To further build upon the diversity of deconstructable PE materials, it would be advantageous to explore alternative cleavable bonds to achieve orthogonal properties and potentially enable new pathways for chemical recycling.

Here, we introduce linear HDPE containing Si–O linkages, specifically, bifunctional silyl ethers (BSEs), i.e., SiR_2-(OR'_2). BSEs combine excellent thermal stability with the capability to undergo selective cleavage on demand.[6,32–37] Additionally, the Si substituents of BSEs can be tuned, leading to variable properties such as Si–O bond hydrolytic cleavage rate.[34,36,38,39] First, we develop conditions for the catalytic ROMP of BSE-containing cyclic olefins in the presence of cyclooctene,[19,26,40] which following hydrogenation enables access to BSE-based HDPE of variable molecular weight. We show that these Si–O containing materials have crystal structures and thermal stabilities similar to commercial HDPE, and that their crystallinities can be tuned by varying the BSE concentration or the Si substituents (e.g., ^{i}Pr versus Et). We demonstrate two routes for chemical recycling of these materials: first, using selective Si–O bond cleavage to produce oligomeric diols suitable for repolymerization; and second, through octanoic acid-catalyzed Si–O bond exchange using propanol. We show that these step-growth repolymerization reactions generate recycled BSE-based HDPE with molar masses nearly identical to the parent sample, despite their fundamental differences in polymerization mechanism. Finally, we show that BSE-based HDPE and its chemically recycled products display tensile properties on par with commercial HDPE, suggesting that they could be used as HDPE substitutes in high-value applications.

Results and Discussion

Synthesis of BSE-Containing PE Mimics

The copolymerization of a cyclic hydrocarbon with a cleavable comonomer via ROMP, followed by hydrogenation of the copolymer backbone, is an established strategy to produce HDPE-like materials;[19] however, most previous reports use a stoichiometric amount of initiator (e.g., 1 equiv. of Grubbs 1st or 2nd-generation complex per polymer chain), which leads to high metal content, and/or perform hydrogenation in a second step, which may add cost and time.[41] Additionally, chemical recyclability of such polymers has not been demonstrated, nor have their tensile properties been directly compared to commercial HDPE. Here, we developed a protocol using a chain transfer agent —*cis*-4-octene— and an in situ hydrogenation process to access PE-mimics in one pot with low loadings of ROMP initiator (0.004 mol %).[42] BSE-based monomers with Et or ^{i}Pr Si-substituents (**EtSi8** or **^{i}PrSi8**) were synthesized according to literature protocols; copolymerization of these monomers with cyclooctene (CO) via ROMP was investigated (Scheme 1).[38] Three copolymers with varied BSE content were synthesized using each BSE comonomer to give 6 polymers in total (CO/RSi8 = 10, 50, 100, Scheme 1, Table 1) following the same general procedure: CO, *cis*-4-octene CTA (0.33 mol % relative to the moles of alkenes; $[RSi8 + CO]_0$:[CTA] = 300), and BSE comonomer were dissolved in 2-methyltetrahydrofuran (2-MeTHF; 1 M relative to the total monomer concentration) under inert atmosphere; Grubbs 3rd-generation bis-pyridyl complex (0.004 mol % relative to the moles of alkenes; $[RSi8 + CO]_0$:[G3] = 25,333) was added and the reactions were stirred at room temperature for 2 h. Quantitative conversions of both monomers and complete BSE incorporation were observed by NMR spectroscopy (Figures S1–S4). The reactions were quenched with excess ethyl vinyl ether. While the resulting Fischer carbenes have been shown to be active hydrogenation catalysts at high hydrogen pressures,[40,43,44] we found that adding a small amount (0.1 mol % relative to the moles of alkenes; $[RSi8 + CO]_0$: [Cat.] = 1,000) of Wilkinson's chlorotris(triphenylphosphine)rhodium(I) complex directly to the crude reaction mixture enabled complete hydrogenation under less energy-intensive conditions (room temperature in 24 h using 1 atm H_2).

The hydrogenated copolymer products precipitated from 2-MeTHF, allowing for collection without the need for further purification. Successful hydrogenation was confirmed by Fourier Transform Infrared (FTIR) and NMR spectroscopies, which showed disappearances of the C=C bending feature at 1603 cm^{-1} (Figure S5) and olefinic proton resonances (Figures S6–S9), respectively. Size exclusion chromatography yielded molar masses of ≈40 kDa for all

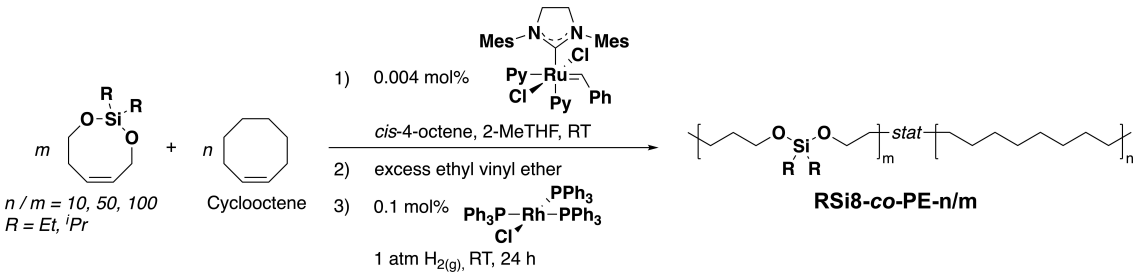

Scheme 1. One-pot synthesis of BSE-based HDPE mimics. Py = pyridine; Mes = mesityl; RT = room temperature.

Table 1: Yields and properties of BSE-based HDPE mimics.

Entry	(Co)polymer[a]	Yield [%]	M_n [kDa][b]	$Đ$[b]	T_m [°C][c]	$\triangle H_m$ [J g^{-1}][d]	$X_{c,\ DSC}$ [%][d]	$X_{c,\ XRD}$ [%][e]	L [Å][f]
1	**^{i}PrSi8-*co*-PE-10**	82	37.3	2.66	86	100	34	34.0	124
2	**^{i}PrSi8-*co*-PE-50**	85	42.3	2.19	91	117	40	37.0	132
3	**^{i}PrSi8-*co*-PE-100**	86	42.5	2.32	92	124	42	42.3	133
4	**EtSi8-*co*-PE-10**	75	39.7	2.02	94	145	50	47.3	133
5	**EtSi8-*co*-PE-50**	77	42.9	2.20	104	150	51	47.9	140
6	**EtSi8-*co*-PE-100**	81	43.0	2.13	112	170	58	60.6	145
7	**^{i}PrSi8-*co*-PE-50-HMW**	71	154	2.82	93	106	36	40.0	126
8	**Commercial HDPE**	n.d.	n.d.	n.d.	128	217	74	79.8	171

[a] Value following dash corresponds to the CO/BSE comonomer ratio *n/m*. [b] Number-average molar masses and dispersities were determined by size-exclusion chromatography in $CHCl_3$ by comparison to low dispersity polystyrene standards. [c] Determined by DSC thermogram (exo up, 10 °C min^{-1}, second run). [d] Relative to 100% crystalline PE ($\triangle H_m = 293$ J g^{-1}). [e] Determined by the ratio of crystalline XRD features (110 and 200) to amorphous XRD features. [f] The average lamellar thickness calculated with the Scherrer equation for 110 and 200 diffraction peaks. n.d. = not determined.

samples and dispersities ranging from 2–2.7, which agrees well with other reported examples of ROMP-based HDPE-like materials (Table 1). We noted that these molar mass values are below those of typical commercial HDPE, and thus we set out to tune these reaction conditions to obtain a higher molar mass material suitable for mechanical property testing. By shortening the reaction time to 10 min, which limits backbiting, and reducing the reaction concentration to 0.5 M to compensate for the decreased solubility of longer aliphatic chains, copolymer **^{i}PrSi8-*co*-PE-50-HMW** with a molar mass of 154 kDa was obtained (Table 1, Figures S10–S11).

Structure and Stability of BSE-Containing PE Mimics

Thermal gravimetric analysis (TGA) was used to assess the thermal stability of these BSE-based HDPE samples under ambient atmosphere. While many studies of ROMP-derived PE-like materials have not investigated thermal stability, Wurm and co-workers reported that PE mimics with orthoester backbone linkages displayed a decomposition temperature >100 °C less than that of HDPE.[19,45] We hypothesized that the high bond dissociation enthalpy of Si–O bonds may impart good thermal stability to BSE-based PE mimics. In support of this hypothesis, our samples displayed decomposition temperatures within ≈10–20 °C of commercial HDPE even at the highest BSE concentration (Figure 1a, Figure S12), with Et-substituted samples showing lower thermal stability compared to their ^{i}Pr counterparts, which may be due to their lower hydrolytic stability. The slightly reduced stabilities of our materials compared to HDPE may be due to the presence of residual Ru, hydrolytic cleavage of the BSEs, or differences in the molar masses, and therefore chain end density, of the two samples.

The melting temperatures (T_m) and degrees of crystallinity ($X_{c,\ DSC}$) of each material were determined by differential scanning calorimetry (DSC). As expected, both values increased as the amount of BSE decreased (Figure 1b–c, Table 1), regardless of the BSE identity. The steric bulk of the Si substituents also had a significant impact on T_m and $X_{c,\ DSC}$, as has been observed for related orthoester-based PE mimics.[19] For example, **EtSi8-*co*-PE-10** displayed a T_m at 94 °C and 49.5% crystallinity, while the ^{i}Pr analog at the same BSE concentration, **^{i}PrSi8-*co*-PE-10**, displayed a T_m at 86 °C and only 34.1% crystallinity. Similarly, **EtSi8-*co*-PE-100** had a T_m at 112 °C and 58.1% crystallinity, while **^{i}PrSi8-*co*-PE-100** had a T_m at 92 °C and 42.3% crystallinity (Figure 1b, Table 1). *I.e.*, for PE mimics with the same BSE concentration, the Et-substituted samples consistently exhibited higher melting temperatures and crystallinities than ^{i}Pr-substituted samples (Figure 1c), presumably because the smaller Et substituents do not perturb the hairpin crystal structure of PE to the same extent as ^{i}Pr. Compared to its smaller molar mass counterpart, **^{i}PrSi8-*co*-PE-50-HMW** displayed a slightly higher T_m (93 °C) and slightly lower crystallinity (36.2%). The latter observation is believed to result from entanglement, which can limit crystallization.[46]

Powder X-ray diffraction (PXRD) was used to further support these DSC studies and compare the structures of our materials to HDPE. All samples displayed peaks at similar $2Q$ values compared to HDPE, indicative of analogous orthorhombic crystal structures (Figure S13). The degrees of crystallinity measured by PXRD ($X_{c,\ XRD}$) were determined by Voigt deconvolution of the amorphous scattering from the crystalline peaks (Figures S14—S20); the $X_{c,\ XRD}$ values are in excellent agreement with $X_{c,\ DSC}$ values (Table 1). As expected, the intensities of the PXRD peaks also correlate with $X_{c,\ XRD}$.[19,47]

Lamellar thicknesses (L) were calculated according to the Scherrer equation (Equation 1) where K is a shape factor (taken to be 0.9), λ is the X-ray wavelength, β is the line broadening at half the maximum intensity, and θ is the Bragg angle.[48,49]

$$L = \frac{K\lambda}{\beta cos\theta} \tag{1}$$

For both ^{i}Pr and Et-substituted materials, the L increased as the BSE concentration decreased (Figure 1c–d, Table 1). Moreover, L ranged from 124–133 Å for ^{i}Pr-basd samples and 133–145 Å for Et-based samples. This observation is consistent with the bulkier BSE functional groups being expelled from the crystalline HDPE-like regions

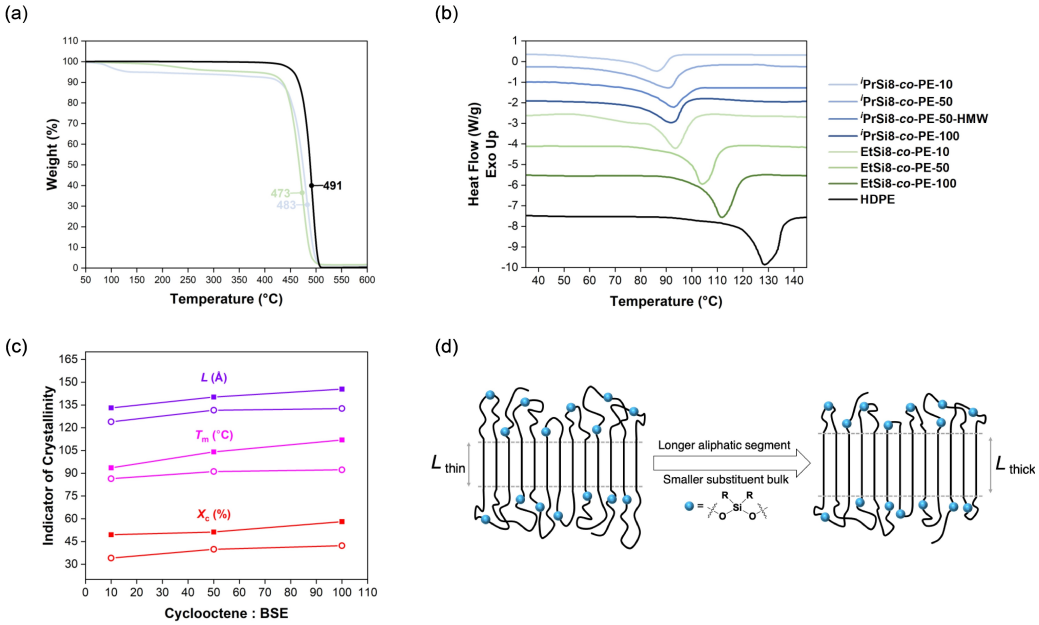

Figure 1. Characterization of thermal and crystalline properties. (a) TGA thermograms for **^{i}PrSi8-*co*-PE-10** (light blue), **EtSi8-*co*-PE-10** (light green), and HDPE (black). T_{decomp}, as measured by the minimum of the first derivative of weight as a function of time, is indicated. (b) DSC thermograms for **^{i}PrSi8-*co*-PE** (blue series), **EtSi8-*co*-PE** (green series) and HDPE (black) (exo up, 10 °C min^{-1}, second run). (c) Melting temperature (T_m), crystallinity (X_c, from DSC), and lamellar thickness (L, from XRD) as a function of the comonomer ratio for **^{i}PrSi8-*co*-PE** (open circles) and **EtSi8-*co*-PE** (closed squares). (d) Schematic of lamellar thickening as the distance between BSEs increases and/or the BSE substituent bulk decreases.

(Figure 1d).[50] Altogether, these results demonstrate that both the BSE concentration and Si substituents of BSEs can be leveraged to tune and potentially optimize the crystallinity of PE mimics for future applications.

Chemical Deconstruction and Recycling of BSE-Based HDPE Mimics

Polymers containing BSEs can undergo selective Si–O bond cleavage in the presence of chemical triggers such as acids and fluoride.[33,34,38] To demonstrate controlled deconstruction of our BSE-based HDPE mimics, each copolymer was exposed to 0.5 M acetic acid in toluene or 0.2 M tetrabutylammonium fluoride (TBAF) in THF and heated for 2 h to 80 °C or 60 °C, respectively (Figure 2a, top). Regardless of the BSE concentration, both sets of conditions led to successful deconstruction as observed by SEC (Figure 2b, dashed and dotted traces). The materials with the highest comonomer ratios (**^{i}PrSi8-*co*-PE-10** and **EtSi8-*co*-PE-10**) decreased in size by more than an order of magnitude following deconstruction (from M_n ≈37.3 to 1.78 kDa and from M_n ≈39.7 to 1.52 kDa, respectively; Table S1). The sizes of the cleavage products decreased as the amount of BSE increased, while samples with the same BSE concentration but different Si substituents produced similarly-sized deconstruction products (Table S1). This observation suggests that **EtSi8** and **^{i}PrSi8** are comparably distributed along the copolymer backbones.

Next, we sought to demonstrate chemical recycling of these BSE-based materials. We note that for both acid- and fluoride-mediated Si–O bond cleavage, the deconstruction products are a mixture of telechelic diols and mono-alcohols. Thus, it is theoretically possible to repolymerize these fragments via step-growth polycondensation to give new BSE-based PE mimics. Moreover, we recently introduced a theoretical model that suggests that step-growth repolymerization of such fragments can, in principle, produce recycled polymers of similar molar mass compared to the parent polymer;[51] however, this model has not been tested in the context of PE-related materials or BSE-containing polymers. Thus, it remains unknown if the products of chain-growth derived ROMP polymers can be repolymerized by step-growth polymerization to give polymers with similar properties. To test this concept, we exposed the acetic acid-generated cleavage products of **^{i}PrSi8-*co*-PE-50** to dichlorodiisopropylsilane in a 1:1 ratio and imidazole in dichloromethane solvent. The conversion of hydroxy groups was measured by monitoring the adjacent methylene protons (H^{a}) compared to 1,3,5-trimethoxybenzene internal standard by ^{1}H NMR spectroscopy (Figures S21–S22). Repolymerization was confirmed by disappearance of the proton H^{a} resonance (Figures S23–S24) and by reformation of high molar mass material by SEC (Figure 2c, dark purple trace). The molar mass of the recycled copolymer (41.6 kDa) was very similar to that of the original **^{i}PrSi8-*co*-PE-50** (42.3 kDa), supporting our theoretical model and confirming successful chemical recycling of chain-growth derived BSE-containing polymers via step-growth repolymerization.

Encouraged by these results, but cognizant of the fact that using a dichlorosilanes for repolymerization does not constitute a fully "closed-loop" process due to the need for

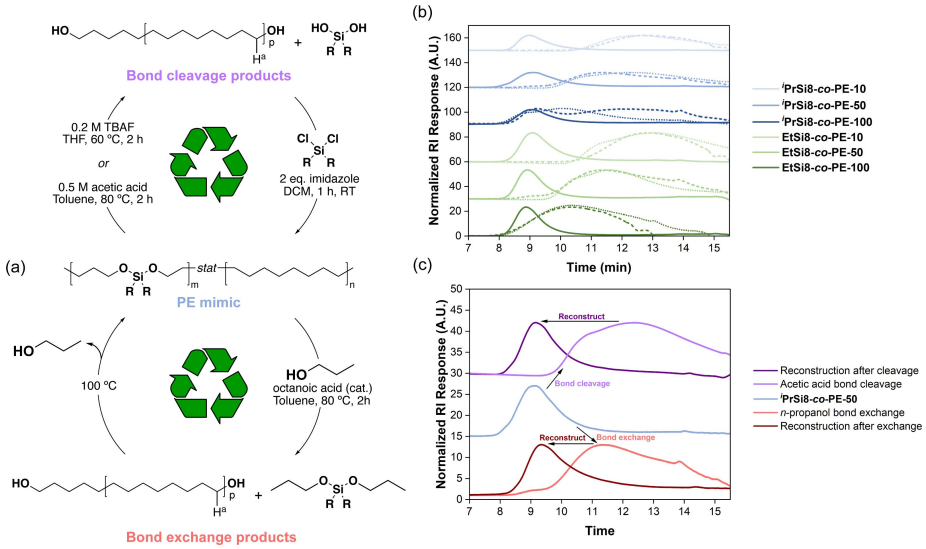

Figure 2. Dual recycling strategies for PE mimics. (a) Scheme depicting acid- or fluoride-triggered bond cleavage followed by repolymerization with dichlorosilane (top) and octanoic-acid catalyzed bond-exchange with *n*-propanol and subsequent repolymerization by removal of *n*-propanol (bottom). (b) SEC traces (normalized RI) of original copolymers (solid traces), copolymers after TBAF treatment (dashed traces), and copolymers after acetic acid treatment (dotted traces) for **^{i}PrSi8-*co*-PE** (blue series) and **EtSi8-*co*-PE** (green series). (c) SEC traces (normalized RI) of original **^{i}PrSi8-*co*-PE-50** (medium blue trace), **^{i}PrSi8-*co*-PE-50** after acetic acid cleavage and subsequent reconstruction (purple traces), **and ^{i}PrSi8-*co*-PE-50** after bond exchange and subsequent reconstruction (red traces).

new silane monomers in each cycle, we sought an alternative route to chemical recycling of these systems that leverages the dynamic covalent chemistry of Si–O bonds.[52] While precedent for acid-catalyzed Si–O bond exchange was established in polydimethylsiloxanes as early as the 1950s and has since been leveraged for reprocessing of various thermosetting systems, to our knowledge, this reactivity has not been used to execute a chemical recycling strategy.[52–56] To demonstrate this idea, **^{i}PrSi8-*co*-PE-50** was treated with a large excess of *n*-propanol (>100 equiv. per BSE) in toluene in the presence of a catalytic amount of octanoic acid at 80 °C. These conditions facilitated an Si–O bond exchange reaction between *n*-propanol and the BSEs in the **^{i}PrSi8-*co*-PE-50** backbone, yielding hydroxy-terminal deconstruction products and diisopropyldipropoxysilane (Figure 2a, bottom, Figures S25–S26). SEC reveals that this process deconstructs the copolymer backbone to a similar extent as acid or fluoride-mediated bond cleavage (Figure 2c, light red trace, Table S1). An advantage of the bond exchange approach, however, is that reconstruction of the backbone can be achieved by simply exposing the diol products to diisopropyldipropoxysilane and increasing the reaction temperature above the boiling point of *n*-propanol (100 °C) to drive off *n*-propanol and favor repolymerization. Following complete removal of *n*-propanol, proton H^{a} is no longer present in the ^{1}H NMR spectrum, suggesting full conversion back into a copolymer (Figure S27). SEC further shows nearly complete recovery of high molar-mass material upon repolymerization (39.6 kDa, Figure 2c, dark red trace, Table S1). These results show that it is possible to chemically recycle these polymers via a thermal equilibrium with an alcohol in the presence of an acid catalyst (octanoic acid), thereby avoiding the need for fresh silane reagent.

Large-scale recycling efforts are typically preceded by sorting of mixed plastic waste streams with either mechanical or sink-flow density separation techniques.[57] Commodity polyolefins, namely polypropylene (PP), PE, and poly(ethylene terephthalate) (PET) comprise more than half of the plastic waste stream.[58] Thus, it may be advantageous to leverage the selective Si–O bond cleavage of our materials to facilitate their separation from these polyolefins. To demonstrate this concept, pieces of commercial isotactic PP (food storage container), HDPE (squeeze bottle cap), PET (water bottle), and **^{i}PrSi8-*co*-PE-50** were subjected to the acid-mediated deconstruction conditions used above for our PE mimics (Figure 3a). While **^{i}PrSi8-*co*-PE-50** dissolved within 2 h, the PP, HDPE, and PET segments were recovered with no significant mass loss (Figure 3b). The HDPE surface appeared slightly discolored after extended contact with these conditions, but given the minimal change in mass, negligible leeching or dissolution were observed. Successful separation was further confirmed by NMR analysis of the post-deconstruction solution, which matched spectra of the diols obtained for **^{i}PrSi8-*co*-PE-50** deconstruction (Figures S28–S29). Characteristic features corresponding to dissolution of the commodity plastics (e.g., PET resonances at approximately 4.8 and 8.1 ppm in the ^{1}H NMR spectrum) were not observed.

Mechanical Properties of BSE-Containing PE Mimics

Finally, we set out to compare the mechanical properties of our BSE-based HDPE materials to commercial HDPE. We note that commercial HDPE typically has a much larger molar mass (e.g., 100–300 kDa)[59] than our ≈40 kDa PE

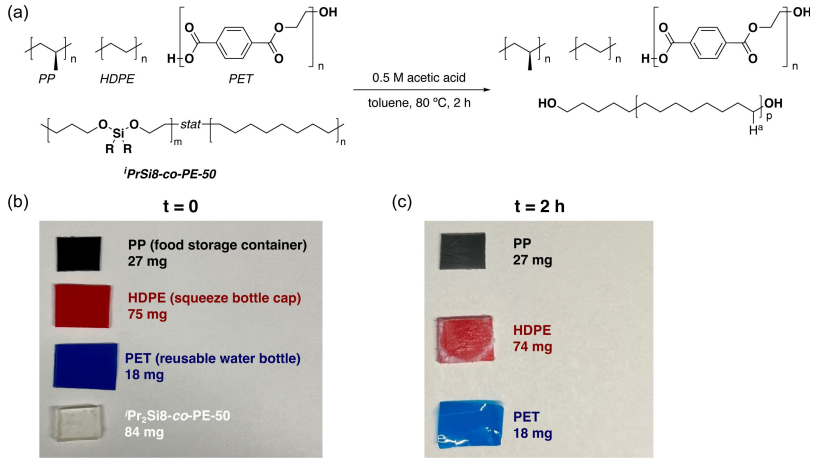

Figure 3. Selective deconstruction of HDPE mimics in the presence of mixed consumer plastics. (a) Scheme depicting acid-mediated deconstruction of **^{i}PrSi8-*co*-PE-50** in the presence of isotactic polypropylene (PP), HDPE, and polyethylene terephthalate (PET). (b) Image of pieces of PP (black), HDPE (red), PET (blue), and **^{i}PrSi8-*co*-PE-50** (clear) before exposure to acetic acid. (c) Image of pieces of PP (black), HDPE (red), and PET (blue) after exposure to acetic acid for 2 h.

mimics, and indeed, tensile tests of the latter revealed substantially lower Young's moduli (≈5 MPa) and strain-at-break values (≈125 %) compared to HDPE (Figures S30–S31). As noted above, however, by tuning the ROMP reaction conditions, a high molecular weight sample, **^{i}PrSi8-*co*-PE-50-HMW**, with a number-average molar mass of 154 kDa (theoretical M_n ≈160 kDa) (Table S1) could be prepared. This copolymer was subjected to the same acid-mediated Si–O bond cleavage and subsequent step-growth repolymerization conditions as described above to generate a recycled sample of nearly equivalent molar mass (Figure S32). The original and recycled materials were then compared to commercial HDPE via shear rheology and tensile tests.

No statistical differences in the storage moduli (G') were observed between **^{i}PrSi8-*co*-PE-50-HMW**, recycled **^{i}PrSi8-*co*-PE-50-HMW**, and HPDE (Figure 4a, Table 2, Figures S33–S35). Likewise, there was no observable difference in

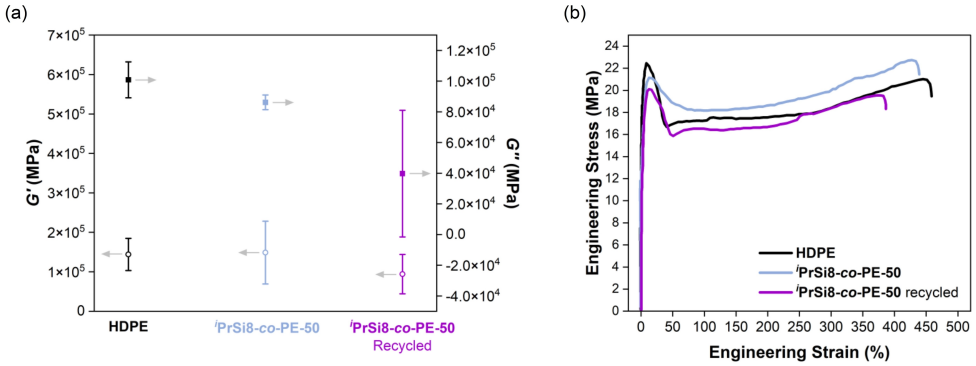

Figure 4. Bulk properties of HDPE and BSE-based HDPE mimics. (a) Storage and loss moduli for HDPE (black), **^{i}PrSi8-*co*-PE-50** (blue), **^{i}PrSi8-*co*-PE-50** recycled (purple) from oscillatory rheology. Center values denote average. Error bars denote standard deviation. (b) Representative tensile testing results for HDPE (black), **^{i}PrSi8-*co*-PE-50** (blue), **^{i}PrSi8-*co*-PE-50** recycled (purple) obtained at room temperature with a strain rate of 0.1 mm s^{-1}.

Table 2: Bulk mechanical properties of PE mimics.

(Co)polymer	G' [MPa][a]	G'' [MPa][a]	E [MPa][b]	σ_y [MPa][b]	Strain-at-break [%][b]
HDPE	0.144 ± 0.041	0.101 ± 0.012	661 ± 49.3	22.1 ± 0.37	461 ± 8.01
^{i}PrSi8-*co*-PE-50	0.149 ± 0.079	0.086 ± 0.005	494 ± 51.2	21.2 ± 0.27	430 ± 15.7
^{i}PrSi8-*co*-PE-50 recycled	0.094 ± 0.050	0.040 ± 0.041	451 ± 116	19.1 ± 0.92	397 ± 33.9

[a] Determined by oscillatory rheometry at 0.1 % strain and 10 rad s^{-1}, N = 2. [b] Determined by tensile tensing experiments with a strain rate of 0.1 mm s^{-1}, N = 3.

the loss moduli (G'') between **^{i}PrSi8-*co*-PE-50-HMW** and HDPE. Recycled **^{i}PrSi8-*co*-PE-50-HMW** was found to have a slightly lower loss modulus as well as a larger spread among recorded G'' values, though the overall magnitudes were similar.

While the measured Young's modulus of HDPE (E = 661 MPa) was modestly higher than that of either **^{i}PrSi8-*co*-PE-50-HMW** (E = 491 MPa) or recycled **^{i}PrSi8-*co*-PE-50-HMW** (E = 451 MPa), all values were within the expected range for HDPE materials (Figure 4b, Table 2, Figure S36).[60] Likewise, all three samples were found to have similar yield strengths (σ_y = 19.1–22.1 MPa) and strains-at-break (397–461 %). Thus, our Si–O-containing HDPE displays mechanical properties on par with HDPE, and it can be deconstructed and recycled to give materials that also are similar to HDPE. These findings represent an advance for ROMP-derived PE mimics, as previous studies have found that such materials are either unsuitable for tensile testing or mechanically weak compared to HDPE.[19,21] Moreover, previous studies have not demonstrated chemical recycling of such polymers.

Conclusion

In summary, we report the synthesis of HDPE mimics containing Si–O bonds by a one-pot, sequential ROMP and hydrogenation process that leverages low loadings of Grubbs catalyst (0.004 mol %) and mild hydrogenation conditions (0.1 mol% Wilkinson's complex, 1 atm, room temperature). The polymers display thermal stability on par with HDPE, while the concentration of BSE units and the steric bulk around each silicon atom influence the melting temperatures, crystallinities, and lamellar thicknesses of the copolymers, providing tunable handles to control processing parameters. Our method enables the synthesis of the highest-reported molecular weights for ROMP-derived HDPE mimics, which provides the first examples of such materials with mechanical properties on par with commercial HDPE. Tuning these parameters in tandem allowed us to synthesize copolymers with HDPE-like thermomechanical properties (T_m = 91 °C, X_c = 40 %, E = 494 MPa, σ_y = 21 MPa). Our HDPE mimics are shown to undergo mild, selective backbone deconstruction upon either Si–O bond cleavage or catalytic exchange, and the resulting deconstruction products can be repolymerized via step-growth polymerization to yield recycled materials with nearly the same chemical structure and molar mass as the original material. This deconstruction strategy can be used to separate our HDPE mimics from commodity polyolefins in waste streams including PP, PET, and HDPE. The approach described here showcases how ROMP is a powerful tool for the synthesis of HDPE mimics of high molar mass and tunable functional group density, demonstrates how silyl ethers may expand the available compositions of such materials, and provides novel applications of BSE exchange reactions (e.g., for chemical recycling). Looking forward, step-growth repolymerization of telechelic oligomers into PE-like materials, which is demonstrated here for diols but could potentially be achieved for other functional oligomers generated from PE pyrolysis,[61] could provide a "closed-loop" solution to PE waste.

Acknowledgements

This work was supported by the NSF Center for the Chemistry of Molecularly Optimized Networks (MONET, Award no. 2116298) and the National Science Foundation Graduate Research Fellowship (NSF-GRFP, Grant no. 2141064).

Conflict of Interest

The authors declare no conflict of interest.

Data Availability Statement

The data that support the findings of this study are available from the corresponding author upon reasonable request.

Keywords: Closed Loop Recycling · Green Chemistry · Polyethylene Mimic · Ring-Opening Polymerization · Silyl Ether

[1] J. R. Jambeck, R. Geyer, C. Wilcox, T. R. Siegler, M. Perryman, A. Andrady, R. Narayan, K. L. Law, *Science* **2015**, *347*, 768–771.
[2] L. Yuan, C. Tang, *Chem* **2021**, *7*, 847–848.
[3] J. Scheirs, W. Kaminsky, *Feedstock Recycling and Pyrolysis of Waste Plastics: Converting Waste Plastics into Diesel and Other Fuels*, Wiley, Chichester, **2006**.
[4] K. M. Van Geem, *Science* **2023**, *381*, 607–608.
[5] C. Jehanno, J. W. Alty, M. Roosen, S. De Meester, A. P. Dove, E. Y. X. Chen, F. A. Leibfarth, H. Sardon, *Nature* **2022**, *603*, 803–814.
[6] P. Shieh, M. R. Hill, W. Zhang, S. L. Kristufek, J. A. Johnson, *Chem. Rev.* **2021**, *121*, 7059–7121.
[7] F. Stempfle, P. Ortmann, S. Mecking, *Chem. Rev.* **2016**, *116*, 4597–4641.
[8] W. H. Carothers, *Collected Papers of Wallace Hume Carothers on High Polymeric Substance*, Interscience Publishers, New York, **1940**.
[9] J. Trzaskowski, D. Quinzler, C. Bährle, S. Mecking, *Macromol. Rapid Commun.* **2011**, *32*, 1352–1356.
[10] P. Ortmann, I. Heckler, S. Mecking, *Green Chem.* **2014**, *16*, 1816–1827.
[11] D. Quinzler, S. Mecking, *Angew. Chem. Int. Ed.* **2010**, *49*, 4306–4308.
[12] F. Stempfle, P. Ortmann, S. Mecking, *Macromol. Rapid Commun.* **2013**, *34*, 47–50.
[13] J. T. Patton, M. Boncella, K. B. Wagener, *Macromolecules* **1992**, *25*, 3862–3867.
[14] M. D. Watson, K. B. Wagener, *Macromolecules* **2000**, *33*, 3196–3201.
[15] M. D. Watson, K. B. Wagener, *Macromolecules* **2000**, *33*, 8963–8970.
[16] M. D. Watson, K. B. Wagener, *Macromolecules* **2000**, *33*, 5411–5417.

[17] K. Nomura, N. W. Binti Awang, *ACS Sustainable Chem. Eng.* **2021**, *9*, 5486–5505.
[18] T. Zeng, W. You, G. Chen, X. Nie, Z. Zhang, L. Xia, C. Hong, C. Chen, Y. You, *iScience* **2020**, *23*, 100904.
[19] T. Haider, O. Shyshov, O. Suraeva, I. Lieberwirth, M. Von Delius, F. R. Wurm, *Macromolecules* **2019**, *52*, 2411–2420.
[20] P. Hodge, S. D. Kamau, *Angew. Chem. Int. Ed.* **2003**, *42*, 2412–2414.
[21] Z. Xue, M. F. Mayer, *Soft Matter* **2009**, *5*, 4600–4611.
[22] R. J. Conk, S. Hanna, J. X. Shi, J. Yang, N. R. Ciccia, L. Qi, B. J. Bloomer, S. Heuvel, T. Wills, J. Su, A. T. Bell, J. F. Hartwig, *Science* **2022**, *377*, 1561–1566.
[23] M. Häußler, M. Eck, D. Rothauer, S. Mecking, *Nature* **2021**, *590*, 423–427.
[24] P. Ortmann, T. A. Lemke, S. Mecking, *Macromolecules* **2015**, *48*, 1463–1472.
[25] P. Ortmann, F. P. Wimmer, S. Mecking, *ACS Macro Lett.* **2015**, *4*, 704–707.
[26] T. Steinbach, E. M. Alexandrino, C. Wahlen, K. Landfester, F. R. Wurm, *Macromolecules* **2014**, *47*, 4884–4893.
[27] D. Cam, M. Marucci, *Polymer* **1997**, *38*, 1879–1884.
[28] M. Shen, H. Cao, M. L. Robertson, *Annu. Rev. Chem. Biomol. Eng.* **2020**, *11*, 183–201.
[29] X. Jia, C. Qin, T. Friedberger, Z. Guan, Z. Huang, *Sci. Adv.* **2016**, *2*, e150159.
[30] M. Baur, N. K. Mast, J. P. Brahm, R. Habé, T. O. Morgen, S. Mecking, *Angew. Chem. Int. Ed.* **2023**, *62*, e202310990.
[31] Y. Zhao, E. M. Rettner, K. L. Harry, Z. Hu, J. Miscall, N. A. Rorrer, G. M. Miyake, *Science* **2023**, *382*, 310–314.
[32] A. M. Johnson, K. E. L. Husted, L. J. Kilgallon, J. A. Johnson, *Chem. Commun.* **2022**, *58*, 8496–8499.
[33] P. Shieh, W. Zhang, K. E. L. Husted, S. L. Kristufek, B. Xiong, D. J. Lundberg, J. Lem, D. Veysset, Y. Sun, K. A. Nelson, D. L. Plata, J. A. Johnson, *Nature* **2020**, *583*, 542–547.
[34] K. E. L. Husted, P. Shieh, D. J. Lundberg, S. L. Kristufek, J. A. Johnson, *ACS Macro Lett.* **2021**, *10*, 805–810.
[35] M. C. Parrott, J. C. Luft, J. D. Byrne, J. H. Fain, M. E. Napier, J. M. Desimone, *J. Am. Chem. Soc.* **2010**, *132*, 17928–17932.
[36] J. Szychowski, A. Mahdavi, J. J. L. Hodas, J. D. Bagert, J. T. Ngo, P. Landgraf, D. C. Dieterich, E. M. Schuman, D. A. Tirrell, *J. Am. Chem. Soc.* **2010**, *132*, 18351–18360.
[37] A. Arroyave, S. Cui, J. C. Lopez, A. L. Kocen, A. M. Lapointe, M. Delferro, G. W. Coates, *J. Am. Chem. Soc.* **2022**, *144*, 23280–23285.
[38] P. Shieh, H. V. T. Nguyen, J. A. Johnson, *Nat. Chem.* **2019**, *11*, 1124–1132.
[39] Y. S. AlFaraj, S. Mohapatra, P. Shieh, K. E. L. Husted, D. G. Ivanoff, E. M. Lloyd, J. C. Cooper, Y. Dai, A. P. Singhal, J. S. Moore, N. R. Sottos, R. Gomez-Bombarelli, J. A. Johnson, *ACS Cent. Sci.* **2023**, *9*, 1810–1819.
[40] C. S. Sample, E. A. Kellstedt, M. A. Hillmyer, *ACS Macro Lett.* **2022**, *11*, 608–614.
[41] L. Xia, T. Peng, G. Wang, X. Wen, S. Zhang, L. Wang, *ChemistryOpen* **2019**, *8*, 45–48.
[42] J. B. Matson, S. C. Virgil, R. H. Grubbs, *J. Am. Chem. Soc.* **2009**, *131*, 3355–3362.
[43] K. D. Camm, N. M. Castro, Y. Liu, P. Czechura, J. L. Snelgrove, D. E. Fogg, *J. Am. Chem. Soc.* **2007**, *129*, 4168–4169.
[44] S. D. Drouin, F. Zamanian, D. E. Fogg, *Organometallics* **2001**, *20*, 5495–5497.
[45] M. Eck, S. T. Schwab, T. F. Nelson, K. Wurst, S. Iberl, D. Schleheck, C. Link, G. Battagliarin, S. Mecking, *Angew. Chem. Int. Ed.* **2023**, *62*, e202213438.
[46] W. G. Perkins, N. J. Capiati, R. S. Porter, *Polym. Eng. Sci.* **1976**, *16*, 200–203.
[47] E. Tarani, I. Arvanitidis, D. Christofilos, D. N. Bikiaris, K. Chrissafis, G. Vourlias, *J. Mater. Sci.* **2023**, *58*, 1621–1639.
[48] A. L. Patterson, *Phys. Rev.* **1939**, *56*, 978–982.
[49] P. Scherrer, *Nachr. Ges. Wiss. Goettingen Math.-Phys. Kl.* **1918**, *2*, 98.
[50] J. C. Markwart, O. Suraeva, T. Haider, I. Lieberwirth, R. Graf, F. R. Wurm, *Polym. Chem.* **2020**, *11*, 7235–7243.
[51] G. R. Kiel, D. J. Lundberg, E. Prince, K. E. L. Husted, A. M. Johnson, V. Lensch, S. Li, P. Shieh, J. A. Johnson, *J. Am. Chem. Soc.* **2022**, *144*, 12979–12988.
[52] K. E. L. Husted, C. M. Brown, P. Shieh, I. Kevlishvili, S. L. Kristufek, H. Zafar, J. V. Accardo, J. C. Cooper, R. S. Klausen, H. J. Kulik, J. S. Moore, N. R. Sottos, J. A. Kalow, J. A. Johnson, *J. Am. Chem. Soc.* **2023**, *145*, 1916–1923.
[53] P. Zheng, T. J. McCarthy, *J. Am. Chem. Soc.* **2012**, *134*, 2024–2027.
[54] T. Debsharma, V. Amfilochiou, A. A. Wróblewska, I. De Baere, W. Van Paepegem, F. E. Du Prez, *J. Am. Chem. Soc.* **2022**, *144*, 12280–12289.
[55] Y. Nishimura, J. Chung, H. Muradyan, Z. Guan, *J. Am. Chem. Soc.* **2017**, *139*, 14881–14884.
[56] C. A. Tretbar, J. A. Neal, Z. Guan, *J. Am. Chem. Soc.* **2019**, *141*, 16595–16599.
[57] K. Ragaert, L. Delva, K. Van Geem, *Waste Manage.* **2017**, *69*, 24–58.
[58] Plastic Europe – Association of Plastics Manufactures, *Plast. Eur.* **2020**, 1–64.
[59] J. R. Martin, J. F. Johnson, A. R. Cooper, *J. Macromol. Sci. Part C* **1972**, *8*, 57–199.
[60] D. Jeremic, *Ullmann's Encyclopedia of Industrial Chemistry*, Wiley-VCH, Weinheim, **2014**.
[61] H. Li, J. Wu, Z. Jiang, V. M. Zavala, C. R. Landis, M. Mavrikakis, G. W. Huber, *Science* **2023**, *381*, 660–666.

Manuscript received: October 7, 2023
Accepted manuscript online: October 30, 2023
Version of record online: November 15, 2023